Electromagnetic Safety Assessment of a Cortical Implant for Vision Restoration

Pragya Kosta, *Student Member, IEEE*, Javad Paknahad, *Student Member, IEEE*, Erik Saturnino Gámez Rodríguez, *Member, IEEE*, Kyle Loizos, *Member, IEEE*, Arup Roy, Neil Talbot, Scott Seidman, Proyag Datta, Rongqing Dai, *Member, IEEE*, Bret Pollack, Robert Greenberg, *Senior Member, IEEE*, and Gianluca Lazzi, *Fellow, IEEE*

***Abstract*—A cortical visual prosthetic system bypasses the components of the visual pathway, which may be damaged due to injury or disease, by directly stimulating the visual cortex; therefore, cortical visual prostheses promise the capability of restoring a form of vision to patients who cannot benefit from other types of visual neural stimulators. A high data rate, multielectrode, implantable device, such as that utilized for a cortical visual prosthesis, requires continuous power provided by an external telemetry unit, which is nonnegligible, given the number of stimulating electrodes and the stimulation rate necessary to avoid flickering visual percepts. This aspect motivates the need to develop models and methods that aid the development of such devices by assessing their compliance with electromagnetic safety standards. In this paper, the electromagnetic safety assessment of a cortical visual prosthetic system is considered, and the solutions employed to numerically treat the computational complexities associated with it are discussed. The specifics of the implementation of an actual visual cortical implant are discussed, and the parameters of such an implant are used as a test case to determine whether IEEE and ICNIRP electromagnetic standards are met in what can be considered a typical embodiment of the prosthesis. Results show that, for the considered implant, such a system meets IEEE and ICNIRP safety standards, thus enabling further development of similar neurorehabilitative devices.**

***Index Terms*—Electromagnetics, finite difference methods, implantable biomedical devices, specific absorption rate, visual prosthesis.**

Manuscript received December 6, 2017; revised February 2, 2018; accepted February 7, 2018. Date of publication March 5, 2018; date of current version April 3, 2018. This work was supported by the Second Sight Medical Products, Inc., under Contract 10036941 to the University of Utah. This paper was presented in part at the 2017 IEEE International Symposium on Antennas and Propagation and USNC-URSI Radio Science Meeting, San Diego, CA, USA, July 2017. *(Corresponding author: Pragya Kosta.)*

P. Kosta, J. Paknahad, E. S. Gámez Rodríguez, and K. Loizos are with the Department of Electrical and Computer Engineering, University of Utah, Salt Lake City, UT 84112 USA (e-mail: pragya.kosta@utah.edu; javad.paknahad@utah.edu; erik.gamez@utah.edu; k.loizos@utah.edu).

A. Roy, N. Talbot, S. Seidman, P. Datta, R. Dai, B. Pollack, and R. Greenberg are with the Second Sight Medical Products, Inc., Sylmar, CA 91342 USA (e-mail: arupr@secondsight.com; ntalbot@secondsight.com; sseidman@secondsight.com; pdatta@secondsight.com; rdai@secondsight.com; bpollack@secondsight.com; bobg@secondsight.com).

G. Lazzi is with the Departments of Electrical Engineering and Ophthalmology, University of Southern California, Los Angeles, CA 90089 USA (e-mail: lazzi@usc.edu).

Color versions of one or more of the figures in this paper are available online at http://ieeexplore.ieee.org.

Digital Object Identifier 10.1109/JERM.2018.2812302

I. Introduction

ACCORDING to a recent study [1], an estimated 250 million people have vision impairment globally; among them, 30 million people are blind, and 220 million people have moderate to severe vision impairment. Further, the growth and aging of the world's population is resulting in a significant increase in the number of people affected by partial or total vision loss. Therefore, the research and development of neuroprostheses capable of restoring useful vision to the blind is of great importance.

In a healthy retina, photoreceptors convert light into electric pulses: these electric pulses relate visual information which is processed by retinal cells and ultimately reach the visual cortex via the optical nerve. Damage to any component of the visual pathway can result in partial or complete blindness. Various embodiments of visual prostheses have been proposed to restore some form of vision to the blind; these can follow different approaches, depending upon the component of the visual pathway that is damaged. While retinal degenerative diseases such as Retinitis Pigmentosa (RP) and Age-Related Macular Degeneration (AMD) can be ameliorated through an "artificial retina," which is a prosthetic system that stimulates the surviving retinal cells, damage to other components of the visual pathway require an implant that interfaces with the neural system past the retina. Thus, although retinal prosthetic devices have matured to the point of being commercially available, their use is limited to patients affected by RP or AMD and, consequently, there is a marked need for other visual prosthetic approaches by which a larger number of visually impaired patients can benefit from. Cortical visual prostheses have attracted significant interest precisely because they are intended to directly stimulate the visual cortex, thus bypassing all the components of the visual pathway prior to it [2]. Therefore, if successful, it can be a useful solution to most conditions causing blindness besides RP and AMD, including, for example, glaucoma and diabetic retinopathy. In glaucoma, ocular hypertension causes damage to the optical nerve, leading to loss of vision; diabetic retinopathy causes instead degeneration in ganglion cells and of the optic nerve.

As with any prosthetic system requiring RF power from external devices, one of the major concerns is to ensure the patient's safety when exposed to the electromagnetic fields generated by the external telemetry device [2], [3]. For this reason, the exposure to electromagnetic fields generated by the active components of the prosthetic device must be assessed to ensure that

2469-7249 © 2018 IEEE. Personal use is permitted, but republication/redistribution requires IEEE permission.
See http://www.ieee.org/publications_standards/publications/rights/index.html for more information.

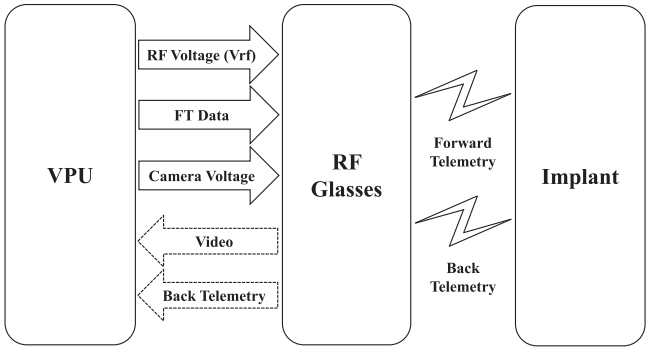

Fig. 1. Block diagram of a cortical visual prosthesis system utilizing glasses with an integrated camera to collect images.

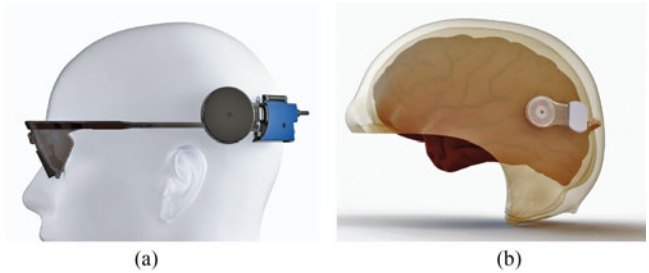

Fig. 2. Orion I clinical system. (a) External components. (b) Implant components.

the radiating device complies with electromagnetic safety standards. Although the models and methods described in this work are widely applicable to any typical cortical visual prosthetic system, we focus on the geometry and parameters of a specific cortical visual prosthetic system currently under development to provide practical findings and report specific observations - the Orion I clinical system [4]. For the numerical simulations, a discretized heterogeneous human head model is used to estimate the fields induced in the tissue. The finite difference time domain (FDTD) method is employed to compute the electromagnetic fields, the Specific Absorption Rate (SAR) of power, and current densities inside the tissue. The electromagnetic fields in and around the location of the implant in the human head are estimated and its compliance with the IEEE safety standards [5] and ICNIRP guidelines [6] is investigated.

The remainder of the paper is organized as follows. Section II introduces a cortical visual prosthetic system and its working principles. Details about the considered numerical model used for safety assessment are presented in Section III. The numerical methods and techniques used in this work are presented in Section IV. Simulation results for the Orion I clinical system and discussions are provided in Section V. Finally, conclusions are provided in Section VI.

II. System Overview

A simple diagram of a cortical prosthesis system is depicted in Fig. 1. This is also the schematic of the visual cortical prosthesis used as an example in this paper-the Orion I system [4]. In general, the wireless link for forward power, forward telemetry (FT) data, and backward telemetry (BT) data is implemented by two inductively coupled coils, placed closely. One of the two coils, the receiving coil, is implanted inside the head; whereas the transmitting coil is external, aligned to the implant coil. There are many possible variations of telemetry systems that have been introduced recently to greatly enhance the coupling between external and internal devices, including the multicoil or metamaterial-based approaches presented in [7]–[10]; nonetheless, for the scope of this paper, we will focus on a traditional two-coil telemetry system. The reasons are two-fold: First, for the most part, the improved telemetry systems tend to result in greater power transfer efficiency and lower SARs, as concluded also in [11], and therefore, a two-coil telemetry system often provides the worst case scenario in terms of induced fields in the tissue, even for well optimized telemetry links; second, the specific embodiment of visual cortical prosthesis that we use as a practical example is being implemented with an optimized two-coil telemetry system, and therefore provides practical parameters utilized in a working system.

The system components can be divided in two categories: the external unit and the implant unit. The external unit comprises a video processing unit (VPU) and RF glasses on top of which a miniature video camera and external (transmitter) coil are mounted. Real time visual data is recorded by the video camera and sent to the VPU, which is worn by the patient. The implantable portion of the system consists of a receiver coil, an array of platinum based electrodes, and the electronic system that provides stimulation current. In the case of the Orion I system, the transmitter and receiver coils are encased in silicone. The electronics package is embedded in a socket which attaches to the skull via bone screws at four locations. The electrode array consists of a polymer cable that contains the conductive wires, which connect to a 60-electrode array. The assembled external parts and the implant device of the Orion I clinical system are shown in Fig. 2(a) and (b), respectively.

III. Simulation Model

For this work, the discretized heterogeneous human head model is derived from the National Library of Medicine (NLM) Visible Man Project [12]. The model is extracted from Magnetic Resonance Imaging (MRI) of a male and has been subsampled at a resolution of 0.25 mm, which we found to be sufficiently accurate to represent the details of the human head and the implant components. As shown in Fig. 3, at this voxel resolution, all external and internal components of the cortical visual prosthetic system considered here (including implant and external coils, socket, cable, array, glasses frame, external coil enclosure, and PCB coils for back telemetry) can be realistically included in the computational grid. However, reducing the simulation space is particularly important given the resolution considered and the low frequency of the telemetry system in order for the problem to be treatable within reasonable computational time. For this reason, the perfectly matching layers (PML) boundary implementation with D-H formulation based FDTD method [13], [14] is utilized to truncate the computational model of the head without incurring in spurious reflections due to the truncation of the head model itself (see Section IV). Thus, the simulation time and space requirements were reduced by only simulating the part of the model essential to affect the fields of the external devices and the fields induced in the tissue: the boundaries of

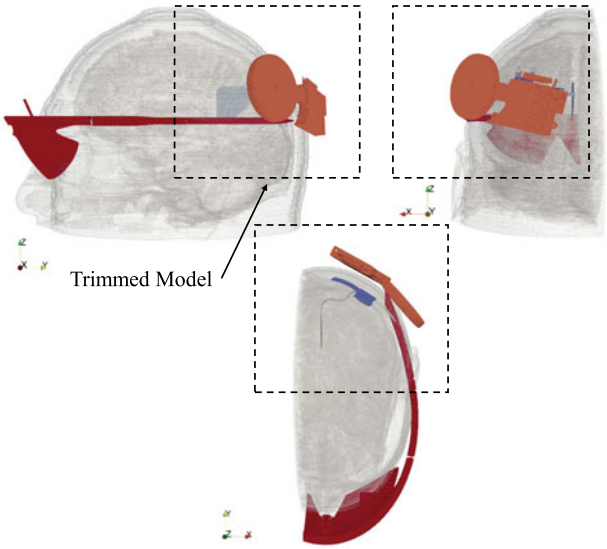

Fig. 3. Numerical human head model.

the final truncated model are indicated in Fig. 3 with dashed lines. The final 0.25 mm resolution model has dimensions of 600 × 525 × 542 computational cells (≈170 million voxels). The dielectric properties and mass densities of various tissues present in the heterogeneous head model and prosthetic system components are taken from [15]–[17] and presented in Table I. To further verify that the final truncated model was indeed sufficient to ensure that the truncation had no meaningful effects on the fields induced in the human head, we utilized a coarse (1 mm resolution) model of whole human head and iteratively reduced the model's boundaries until the effect of the reduction was no longer negligible.

TABLE I
MATERIAL PROPERTIES OF VARIOUS TISSUES AND IMPLANT COMPONENTS AT 3.156 MHZ

Tissue Name	Conductivity [S/m]	Relative Permittivity	Mass Density [Kg/m^3]
Sinus	0	1	1
Cornea	0.790	847	1076
Fat	0.026	20.7	920
Mucous Membrane*	0.296	612	1102
Muscle	0.570	494	1040
Brain White Matter	0.120	279	1043
Gland*	0.673	476	1028
Blood Vessel*	0.333	142	1102
Socket†	7.66×10^6	0	8570
Cable (Gold)	4.56×10^7	0	19320
Array (Gold)	4.56×10^7	0	19320
Foam‡	0	3	1000
External Coil Enclosure	0	3	1070
Glasses Frame	0	8	1550
PCB (FR4)	0	4.4	1850
PCB Coils	5.98×10^7	0	8940
Implant Coil (Gold)	4.56×10^7	0	19320
Implant Coil Insulation§	0	3.5	2330
Cable Insulation§	0	3.5	2330
Cerebellum*	0.234	797	1045
Bone Cortical*	0.032	80.6	1908
Cartilage	0.307	531	1100
Tendon*	0.396	126	1142
Skin Dry	0.067	730	1010
Brain Grey Matter	0.199	554	1039
Lens	0.452	563	1100
Eye Sclera	0.729	691	1170
Blood	0.989	1020	1060
Cerebrospinal Fluid*	2	109	1007
Vitreous Humor	1.5	73.4	1009
Bone Marrow*	0.0057	30.4	1029
Bone Cancellous*	0.103	144	1178

*These properties are obtained from [16].
†The implant component socket is modeled as Niobium.
‡The estimated properties are based on material Polyurethane and [17].
§The coil insulation and cable insulation are modeled as Silicone Rubber.

IV. METHODOLOGY

The FDTD method is a mesh-based numerical modeling method, which is widely used in various fields of science and engineering. The time dependent Maxwell's equations are discretized in time and space using central difference approximations [18]. In continuous-wave simulations, such as those in this paper, the resulting equations are solved in an iterative manner until steady-state is reached [13], [19]. The computational model is terminated with PML boundaries to simulate unconstrained space through reflectionless terminations [20], [21]. In this work, the D-H formulation based FDTD method is used for the field calculations. The D-H formulation of FDTD method has benefit over conventional E-H formulation in that the PML boundary conditions are independent of the background material [14], [22], [23] making it particularly convenient to terminate heterogeneous objects such as the human head model. The use of the FDTD method for this work has several advantages: 1) It uses a rectangular grid and, therefore, readily available voxelized head models can be used; 2) it is computationally very efficient and allows handling/meshing of large heterogeneous models, such as the one considered in this paper; 3) it is amenable for efficient implementation of absorbing boundary conditions suitable for reflectionless truncation of heterogeneous models, which further reduces significantly the simulation time and memory requirements [24].

In the cortical visual prosthetic example considered here, the external coil has an outer diameter of 37.56 mm and a peak coil current of 0.998 A at the operating frequency of 3.156 MHz. The implant coil outer diameter is 18 mm and its peak coil current is 0.099 A for the desired stimulation output. The implant and external coils are separated by a distance of 15 mm. These parameters have been chosen as worst case wireless link between the external and implant devices.

A. Source Excitation

Various methods for source excitation are available in FDTD. A widely used source model, i.e., the "voltage source," can be applied across the inner and outer ends of the spiral coil, although doing so results in unrealistically high electric fields in the region proximal to the voltage source gap, an aspect that is particularly important in this case given the proximity to the scalp of the external transmit telemetry coil. For this reason, the "current source" excitation method is used here, where the external coil is modeled with a constant current at all locations along the coil's wire. The current source can be implemented by

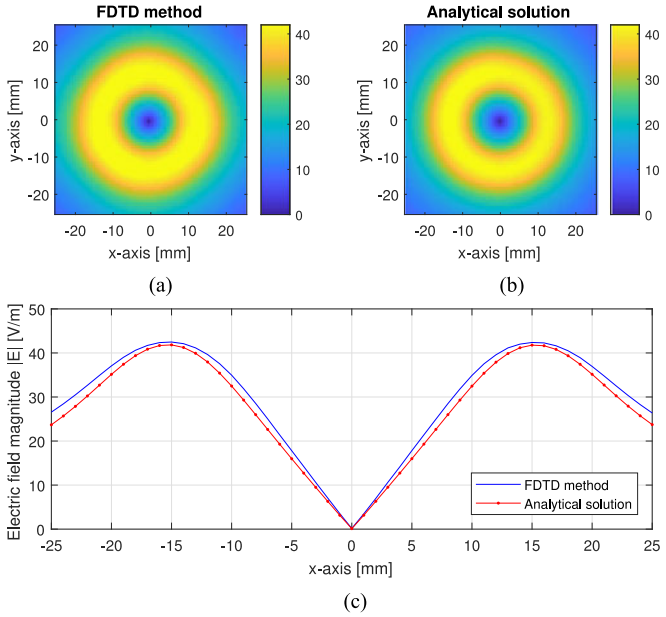

Fig. 4. Electric field magnitude (in V/m) computed from FDTD method and analytical solution. The coil is considered to be in xy-plane with center at the origin. (a) Electric field magnitude |E| in xy-plane and z = 5mm. (b) Electric field magnitude |E| along x-axis, y = 0, z = 5 mm.

either forcing directly the electric field along the coil's wire or the magnetic field surrounding the coil's voxels: both methods provided identical results.

For validation, the electromagnetic fields generated by the coil in absence of the tissue are computed using FDTD and compared with the analytical solutions from [25]. The coil is considered to be in the xy-plane, with center at the origin. The agreement between analytical and FDTD computed fields, shown in Fig. 4, is excellent. The numerical error due to staircasing is localized at the interfaces and leads to some single voxel high values. However, these high values are averaged out during the computation of spatial-average SAR.

B. Coil Modeling

The external coil is modeled as a current source; as shown in Fig. 3, the external coil is parallel to the head and makes an angle with the x-, y-, and z-axes. In order to ensure continuous current path, devoid of short circuits, for the FDTD model of this slanted coil a three-dimensional continuous current path is found along the meshed coil wire and a constant current is forced along this path. The electric field along the current path is initially forced to unity and later scaled to match the coil current to the value of the transmit coil implemented in the actual system.

In the discretized model, the coil current path consists of a series of straight line segments which connects the inner end of the coil to the outer end of the coil. Each segment is a straight line between two vertices of a simulation cell, which is either edge, face diagonal, or body diagonal of the cell; each face diagonal segment is replaced by two side segments on the same face connecting the ends of the diagonal. Similarly, each body diagonal segment is replaced by three side segments connecting the diagonal. In this way, a connecting path between the two ends of the coil with uniform current is created, which contains

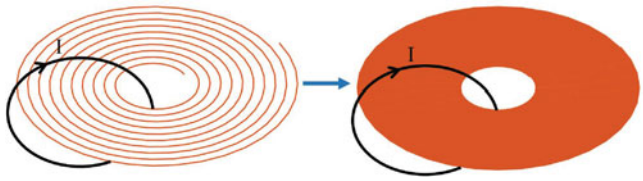

Fig. 5. Homogenized coil implemented in the FDTD mesh.

the straight-line segments parallel to either x-, y-, or z-axis. To model the current source in FDTD, the electric field "hard source" excitation is employed [13]. The x, y, and z components of the electric field corresponding to the side segments are forced to unity. However, components corresponding to face diagonal are weighted down by $1/\sqrt{2}$ and those corresponding to body diagonal are weighted by $1/\sqrt{3}$. The fields generated by the implant coil are significantly smaller compared to the fields generated by the external coil and are therefore neglected here.

C. Homogenized Coil

In order to handle the close spacing between adjacent turns of the coil and overlapping of the turns in the discretized case, the coil is modeled essentially as a homogenized coil (Fig. 5). The total current of this homogenized coil is identical to that of the actual coil. The fields generated by the homogenized coil are validated against the fields of the actual spiral coil, and the error is found to be less than 1%. Ampere's law is used to scale the magnetic field (and, similarly, the electric field) appropriately for the given coil current.

D. Sigmoid Function for DC Offset Elimination

In the FDTD simulations, a DC offset in the computed time domain electric or magnetic fields may occur [26]. For continuous wave (CW) source, this effect can be avoided by multiplying the source excitation waveform by an appropriate ramp function. In this work, we have used a sigmoid function, represented by the following expression:

$$\frac{2}{1+\exp(\alpha\frac{Re(-t)}{Re(nsteps)-1})}$$

where the parameter α represents the sigmoid steepness, $nsteps$ the number of simulation steps in a simulation cycle and t is instantaneous time. For higher values of α, the sigmoid saturates to 1 quickly and thus the simulation requires a lower number of simulation cycles, albeit the downside is the higher likelihood of introducing a DC offset. Conversely, for lower values of α, the sigmoid saturates to 1 slowly and the simulation requires longer simulations to reach steady-state. Considering the tradeoff between simulation time and accuracy of results, in this work, we have used a value of 2.5 for the sigmoid parameter α.

E. Peak Computation

The two-point method is a commonly used technique for finding peak and phase of a sinusoidal waveform by using two sample points at steady state. However, the sample points need to be selected from the simulation cycle for which fields are converged and the modulating sigmoid function is saturated. For

the considered value (2.5) of the sigmoid parameter α, the fields converged in four simulation cycles. Due to the large size of the model (≈170 million cells), it became imperative to optimize the simulation time of the FDTD simulations. To accomplish this, the peak electric and magnetic fields are computed using the Discrete Fourier Transform (DFT) from the first half simulation cycle. Before computing the DFT, the time domain fields samples computed by FDTD simulations were multiplied by the reciprocal of the sigmoid function, in order to neutralize the effect of sigmoid. This weighted DFT method of peak computation is validated against the two-point method and the error is found to be less than 2%. Next, the electric field peak value at each voxel is used to compute the averaged SAR and induced current densities. The procedures for the computation of these quantities are included in following section.

V. Results

A. Averaged 1 g and 10 g SARs

A common approach to estimate the electromagnetic energy absorbed by the body is to compute the average SAR inside the tissue. Although the latest IEEE electromagnetic safety standard [5] calls for testing that the 10 g SAR in the shape of a cube be lower than 2W/kg, previous standards (as well as current standards for wireless devices, albeit these are in a different context) consider a generally more stringent 1 g SAR as well. Thus, for completeness, both will be computed and reported here. In order to calculate the spatial-average 1 g (10 g) SAR in a tissue volume, the mass should be 1 gram (10 gram), with 5% error at most. The spatial-peak 1 g SAR should not exceed 1.6 W/kg for any 1 gram of tissue, and 2 W/kg for any 10 grams in a cubical tissue volume.

The procedure to compute peak spatial-averge SAR is in accordance with the computation guidlines provided in the IEC/IEEE standard for using FDTD for SAR calculations [27]. The volume of the cube has been defined and centered at each voxel of the head model; the number of voxels in all directions is increased until the desired value is obtained for the 1 g or 10 g. When it is not possible to reach 1 g or 10 g mass, the center of the cubical volume is shifted until these are achieved. The cubical volume considered should be entirely inside the model to be a valid volume for SAR computation. Once the suitable volume has been achieved, the averaged 1 g or 10 g SAR can be calculated by adding voxel SARs and dividing by the number of voxels for the desired 1 g (or 10 g) of cube. The voxel SAR is calculated from the electric fields and the material properties of the tissue using the following equation:

$$\text{SAR} = \frac{\sigma\left(|E_{xp}|^2 + |E_{yp}|^2 + |E_{zp}|^2\right)}{2\rho}$$

where σ is the conductivity of the human tissue, ρ is its mass density, and E_{xp}, E_{yp}, and E_{zp}, are peak electric field intensity components along x-, y-, and z-axes respectively. The averaged 1 g and 10 g SAR for the proposed model are shown in Fig. 6. The left figure shows the numerically computed SAR at the surface of the head and the right figure provides the slice where the maximum averaged SAR was obtained. As it can be seen from the figures, and as expected, the location of largest SAR is close to the surface of the head near the skull and implant coil location. The results are summarized in Table II. Both 1 g and 10 g SAR maximum values are significantly lower than the limits prescribed by current and former IEEE standards.

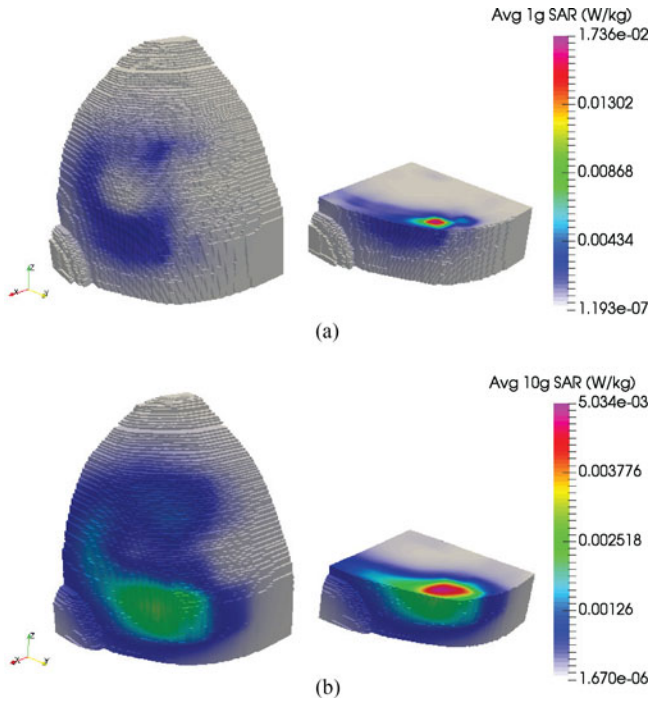

Fig. 6. Averaged 1 g and 10 g SAR [W/kg] for the cortical visual prosthetic under consideration.

TABLE II
AVERAGED SAR

Maximum averaged SAR	Computed values [W/kg]	SAR limit [W/kg]
1 g SAR	0.0174	1.6
10 g SAR	0.0050	2.0

B. Averaged Current Density

At low frequencies, the magnitude of the induced current densities can be a source of concern. The ICNIRP guidelines provide restrictions on both averaged SAR and averaged induced current density for the frequency between 100 kHz to 10 MHz. Based on ICNIRP general exposure recommendations, the induced current density should be averaged over 1 cm^2 inside the body and should be lower than $f/500$ in the frequency range 100 kHz-10 MHz, with f frequency [6].

The induced current densities are obtained from the electric field and conductivity of the tissues according to Ohm's law. Fig. 7 shows the averaged current density in x, y, and z directions respectively. Similar to the SAR results, the averaged current density values are also higher at the location near the skull and close to the internal implant coil. For the specific example considered here, all the components of the current density are in compliance with the limits at the frequency 3.156 MHz (6.3 A/m^2 standard limit). These results are summarized in Table III. All colorbars of Fig. 7 are scaled based

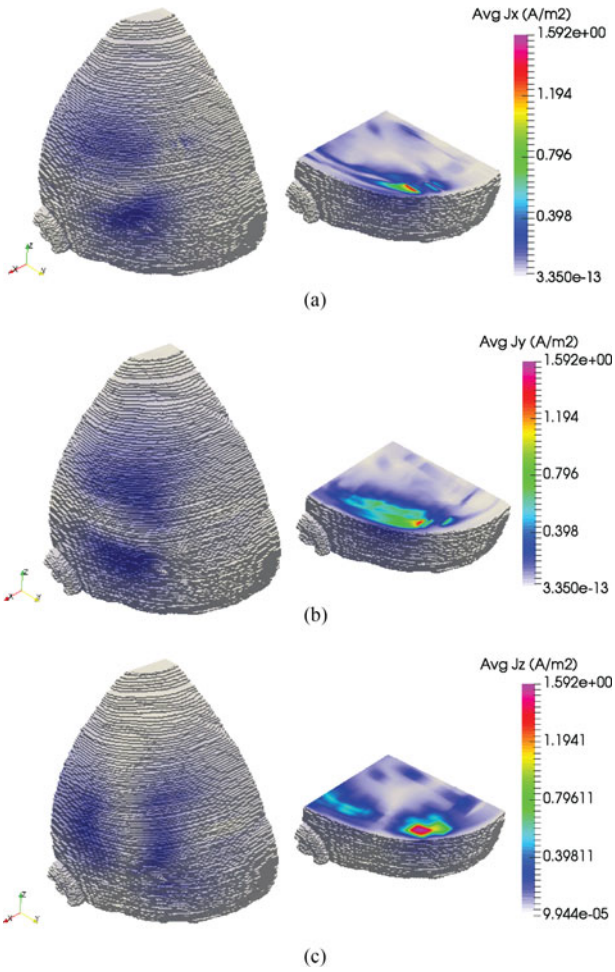

Fig. 7. Averaged current density [A/m^2] (averaged over 1 cm^2 area) for the cortical visual prosthetic under consideration. (a) Jx: x-component of averaged current density [A/m^2]. (b) Jy: y-component of averaged current density [A/m^2]. (c) Jz: z-component of averaged current density [A/m^2].

TABLE III
AVERAGED CURRENT DENSITIES (RMS)

Maximum current densities (averaged over 1 cm^2 area)	Computed values [A/m^2]	Induced current density limit [A/m^2]
Max Avg Jx	1.498	6.3
Max Avg Jy	1.365	6.3
Max Avg Jz	1.592	6.3

on the maximum averaged current density over the x, y, and z directions.

VI. CONCLUSION

In this work, we focused on the electromagnetic safety assessment of a cortical visual prosthesis and used as an embodiment a specific prosthesis currently being developed-the Orion I clinical system [4]. The analysis is performed using a D-H formulation of the FDTD method and the NLM Visible Man head model. For the considered system, the induced current densities and SAR, in the worst-case scenario, are estimated and compared with widely used safety standards, such as IEEE and ICNIRP. The maximum values of estimated averaged 1 g SAR and 10 g SAR (0.017 W/kg and 0.005 W/kg, respectively) are significantly lower than prescribed limits (1.6 W/kg and 2 W/kg, respectively) at the considered frequency of 3.156 MHz. Additionally, the maximum averaged current density is found to be 1.592 A/m^2, which is lower than the ICNIRP guideline limit of 6.3 A/m^2. These findings are important in establishing that the telemetry system for a multielectrode cortical device with high refresh rate, similar to the one considered here, should be in compliance with current guidelines, even for currents in the forward telemetry coil approaching 1 A at the frequency of 3 MHz. Thus, although specific to the Orion I clinical system, the results of this paper furnish a guideline for the development of visual cortical implants, and cortical implants in general.

REFERENCES

[1] R. R. A. Bourne *et al.*, "Magnitude, temporal trends, and projections of the global prevalence of blindness and distance and near vision impairment: A systematic review and meta-analysis," *Lancet Global Health*, vol. 5, no. 9, pp. e888–e897, 2017. [Online]. Available: http://www.sciencedirect.com/science/article/pii/S2214109X17302930

[2] R. A. Normann, E. M. Maynard, K. S. Guillory, and D. J. Warren, "Cortical implants for the blind," *IEEE Spectr.*, vol. 33, no. 5, pp. 54–59, May 1996.

[3] P. Hunter, "Cure for blindness?" *Eng. Technol.*, vol. 4, no. 8, pp. 18–20, May 2009.

[4] 2017. [Online]. Available: http://investors.secondsight.com/news-releases/news-release-details/second-sight-receives-full-fda-approval-begin-first-orion-human

[5] *IEEE Standard for Safety Levels with Respect to Human Exposure to Radio Frequency Electromagnetic Fields, 3 kHz to 300 GHz*, IEEE Std. C95.1-2005, Apr. 2006.

[6] *ICNIRP Guidelines for Limiting Exposure to Time-Varying Electric, Magnetic, and Electromagnetic Fields (up to 300 GHz)*, Health Phys. Std., vol. 74, no. 4, pp. 494–522, Apr. 1998. [Online]. Available: http://www.icnirp.org/cms/upload/publications/ICNIRPemfgdl.pdf

[7] A. K. RamRakhyani and G. Lazzi, "On the design of efficient multi-coil telemetry system for biomedical implants," *IEEE Trans. Biomed. Circuits Syst.*, vol. 7, no. 1, pp. 11–23, Feb. 2013.

[8] A. RamRakhyani and G. Lazzi, "Interference-free wireless power transfer system for biomedical implants using multi-coil approach," *Electron. Lett.*, vol. 50, no. 2, pp. 853–855, Jun. 2014. [Online]. Available: http://digital-library.theiet.org/content/journals/10.1049/el.2014.0567

[9] A. Rajagopalan, A. K. RamRakhyani, D. Schurig, and G. Lazzi, "Improving power transfer efficiency of a short-range telemetry system using compact metamaterials," *IEEE Trans. Microw. Theory Techn.*, vol. 62, no. 4, pp. 947–955, Apr. 2014.

[10] E. S. G. Rodríguez, A. K. RamRakhyani, D. Schurig, and G. Lazzi, "Compact low-frequency metamaterial design for wireless power transfer efficiency enhancement," *IEEE Trans. Microw. Theory Techn.*, vol. 64, no. 5, pp. 1644–1654, May 2016.

[11] A. K. RamRakhyani and G. Lazzi, "Multi-coil approach to reduce electromagnetic energy absorption for wirelessly powered implants," *Healthcare Technol. Lett.*, vol. 1, no. 1, pp. 21–25, 2014.

[12] The National Library of Medicine, "The visible human project," 2000. [Online]. Available: http://www.nlm.nih.gov/research/visible/

[13] D. M. Sullivan, *Electromagnetic Simulation Using the FDTD Method*. Hoboken, NJ, USA: Wiley, 2013.

[14] G. Lazzi, "Unconditionally stable D-H FDTD formulation with anisotropic PML boundary conditions," *IEEE Microw. Compon. Lett.*, vol. 11, no. 4, pp. 149–151, Apr. 2001.

[15] 2017. [Online]. Available: http://niremf.ifac.cnr.it/tissprop/

[16] P. Hasgall *et al.*, "IT'IS database for thermal and electromagnetic parameters of biological tissues," 2015. [Online]. Available: www.itis.ethz.ch/database

[17] T. Blaszczykiewicz, "Breathable neoprene substitute," Mar. 1, 2005, U.S. Patent 6 861 379. [Online]. Available: https://www.google.com/patents/US6861379

[18] K. Yee, "Numerical solution of initial boundary value problems involving maxwell's equations in isotropic media," *IEEE Trans. Antennas Propag.*, vol. AP-14, no. 3, pp. 302–307, May 1966.
[19] A. Taflove and S. C. Hagness, *Computational Electrodynamics: The Finite-Difference Time-Domain Method*, 3rd ed. Norwood, MA, USA: Artech House, 2005.
[20] D. M. Sullivan, "An unsplit step 3-D PML for use with the FDTD method," *IEEE Microw. Guided Wave Lett.*, vol. 7, no. 7, pp. 184–186, Jul. 1997.
[21] G. Lazzi, O. P. Gandhi, and D. M. Sullivan, "Use of PML absorbing layers for the truncation of the head model in cellular telephone simulations," *IEEE Trans. Microw. Theory Techn.*, vol. 48, no. 11, pp. 2033–2039, Nov. 2000.
[22] S. C. DeMarco, G. Lazzi, W. Liu, J. D. Weiland, and M. S. Humayun, "Computed SAR and thermal elevation in a 0.25-mm 2-D model of the human eye and head in response to an implanted retinal stimulator–Part I: Models and methods," *IEEE Trans. Antennas Propag.*, vol. 51, no. 9, pp. 2274–2285, Sep. 2003.
[23] K. Gosalia, J. Weiland, M. Humayun, and G. Lazzi, "Thermal elevation in the human eye and head due to the operation of a retinal prosthesis," *IEEE Trans. Biomed. Eng.*, vol. 51, no. 8, pp. 1469–1477, Aug. 2004.
[24] G. Lazzi, "Computational and experimental bioelectromagnetics for a retinal prosthesis," in *Proc. Int. Conf. Electromagn. Adv. Appl.*, Sep. 2009, pp. 1010–1012.
[25] K. P. Esselle and M. A. Stuchly, "Neural stimulation with magnetic fields: Analysis of induced electric fields," *IEEE Trans. Biomed. Eng.*, vol. 39, no. 7, pp. 693–700, Jul. 1992.
[26] C. M. Furse, D. H. Roper, D. N. Buechler, D. A. Christensen, and C. H. Durney, "The problem and treatment of DC offsets in FDTD simulations," *IEEE Trans. Antennas Propag.*, vol. 48, no. 8, pp. 1198–1201, Aug. 2000.
[27] *IEC/IEEE International Standard - Determining the Peak Spatial-Average Specific Absorption Rate (SAR) in the Human Body From Wireless Communications Devices, 30 MHz to 6 GHz–Part 1: General Requirements for Using the Finite-Difference Time-Domain (FDTD) Method for SAR Calculations*, IEC/IEEE Std. 62704-1, Oct. 2017.

Pragya Kosta (S'15) received the B.Tech. degree in electronics and communication engineering from the Indian Institute of Information Technology, Jabalpur, India, in 2010 and the M.Tech. degree in electronics and communication engineering from the Indian Institute of Technology, Roorkee, India, in 2012. Since August 2015, she has been working toward the Ph.D. degree in electrical engineering at the University of Utah, Salt Lake City, UT, USA.

She was an Assistant Professor with the Department of Electronics and Communication Engineering, Maharana Pratap Group of Institutions, Kanpur, India, and CMR Institute of Technology, Bangalore, India. She has previous research experience in the fields of computational electromagnetics and antenna design. Her current research interests include neuroprostheses, neural stimulation, implantable devices, dosimetry, and bioelectromagnetics.

Ms. Kosta is a frequent Reviewer of the IEEE ANTENNAS AND WIRELESS PROPAGATION LETTERS.

Javad Paknahad (S'14) was born in Iran, in 1989. He received the B.S. degree in electrical engineering from the Amirkabir University of Technology, Tehran, Iran, in 2011 and the M.S. degree in electrical engineering from Shahid Beheshti University, Tehran, in 2013. He is currently working toward the Ph.D. degree in electrical engineering at the Viterbi School of Engineering, University of Southern California, Los Angeles, CA, USA.

He was a Researcher with the Power Quality Laboratory, Sharif University of Technology, Tehran, until 2015. He was also a Graduate Research Assistant with the Department of Electrical and Computer Engineering (ECE), University of Utah, Salt Lake City, UT, USA, from 2016 until the end of 2017. His research interests include biomedical electromagnetics, wireless implantable biomedical systems, and application of electromagnetics in power systems.

Erik Saturnino Gámez Rodríguez (S'13–M'17) was born in El Rosario, Cuscatlán, El Salvador. He received the Bachelor's, M.Sc., and Ph.D. degrees in electrical engineering from the University of Utah, Salt Lake City, UT, USA.

His research interests include wireless power transfer optimization and enhancement, antenna design and miniaturization, novel wireless communication devices, radar imaging, and applications of spatial filtering in the microwave regime.

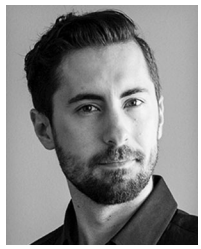

Kyle Loizos (M'10) received the B.S. and M.S. degrees in electrical engineering from the University of Utah, Salt Lake City, UT, USA, in 2014 and the Ph.D. degree in electrical and computer engineering from the University of Utah in 2017.

From 2010 to 2017, he was a Research Assistant with the University of Utah. His research interests include computational modeling of neural tissue and design of neural prosthetic electrodes. He is currently the Director of the Engineering Department, Teveri LLC, Salt Lake City, where he is leading the engineering and design of stretchable electronics for use in textiles and consumer electronics. He has authored or coauthored more than 20 international conference papers, five journal articles, and three patents.

Arup Roy received the B.Tech. degree in instrumentation engineering, with honors, from the Indian Institute of Technology, Kharagpur, India, in 1994; the M.S. degree in biomedical engineering from The Medical College of Virginia, Richmond, VA, USA, in 1996; and the Ph.D. degree in biomedical engineering, from The Johns Hopkins University School of Medicine, Baltimore, MD, USA, in 2007.

As part of his research in the field of computational neuroscience, he investigated whether synchronous firing between neuronal spike trains is affected by the attentional state of nonhuman primates while performing tactile tasks, which ultimately led to the granting of the Ph.D. degree. He is currently the Senior Director of Systems Research and Technology with Second Sight Medical Products, Inc., Developer and Marketer of the Argus II Retinal Prosthesis System and the Orion Cortical Prosthesis System. He has managed and led the design and development effort of numerous production level (for both commercial release and clinical trials) active implantable medical device externals software, hardware, and image processing systems. He has more than 10 peer-reviewed publications and is a named inventor on more than 40 issued patents.

Dr. Roy is a Member of the Association for Research in Vision and Ophthalmology.

Neil Talbot received the B.S. degree as a Regent's Scholar and the M.S. and Ph.D. degrees in mechanical engineering from the University of California at Berkeley, Berkeley, CA, USA, in 1991, 1993, and 1999, respectively.

The emphasis of the Ph.D. research was microfabricated medical devices that led to his position at Second Sight Medical Products, Inc., Sylmar, CA, USA, where he was a key member of the team that developed the first commercial retinal prosthesis. Subsequently at Second Sight, he lead the team that developed the first wireless, chronically implantable, cortical visual prosthesis, which was recently accepted into the FDA Breakthrough Device program. He is co-inventor on 108 patents worldwide (79 US patents) of Second Sight's 350 patents and has three other patents that were filed during his doctoral research. He has been promoted six times at Second Sight and now holds the position of the Senior Director of Implant R&D and Reliability.

Scott Seidman received the B.S.E. degree in engineering science from Tulane University, New Orleans, LA, USA, in 2009 and the M.S. degree in mechanical engineering from San Diego State University, San Diego, CA, USA, in 2015.

He is currently a Research and Development Mechanical Engineer with Second Sight Medical Products, Inc., Sylmar, CA, USA, tasked with developing wirelessly powered implantable systems to cure blindness. His work is focused on next generation external systems for controlling retinal and cortical visual prostheses. Prior to joining Second Sight in 2016, he worked on the development of novel recording electrodes for closed-loop neural-interactive systems to help restore lost function and mobility within NSF funded research.

Proyag Datta received the M.S. degree in mechanical engineering from Louisiana State University, Baton Rouge, LA, USA and the Ph.D. degree from the University of Karlsruhe, Karlsruhe, Germany. He has worked in the field of microtechnology for more than 15 years, during which he designed and fabricated microdevices, developed microfabrication processes, and implemented packaging technologies. He is passionate about the improvement of human life through responsible use of science and technology. He applies his expertise in microtechnology to the development of medical devices.

At Second Sight Medical Products, Sylmar, CA, USA, he works on improving the Argus II retinal prosthesis and on the design and development of the Orion cortical visual prosthesis. As part of the core development team for the Orion prosthesis, he is actively involved in design decisions, fabrication methodology, management of preclinical efforts, and building prototypes for verification and validation.

Rongqing Dai (M'00) received the B.Sc. degree in biomedical engineering from Zhejiang University, Hangzhou, China, and the M.Sc. degree in neuroscience and the M.Eng. degree in electronics and computer engineering from the University of Alberta, Edmonton, AB, Canada.

He was involved in the research and development with Functional Electrical Stimulation (FES) devices for treating spinal cord injuries before joining Second Sight, Sylmar, CA, USA, in 1999, where he is currently the Chief Engineer with the Electrical Engineering Department. He is the Lead Engineer developing the inductive power link, implant coils, and ASICs for implantable visual stimulation devices. His research interests include power control and safety protocols for inductively powered implantable electronic systems.

Bret Pollack received the B.S and M.S. degrees in electrical engineering from the University of Southern California, Los Angeles, CA, USA, in 1990 and 1995, respectively.

Since 1995, he has worked on high-speed analog and mixed signal design, with an emphasis in ultrawideband radio and software defined radio. He is currently a Senior Electrical Engineer with Second Sight Medical devices, Sylmar, CA, USA, specializing in RF communications.

Robert Greenberg (M'87–SM'16) received a degree in technical electronics from the Nassau Technical Institute, Nassau, NY, USA, in 1985; the B.S. degree (*Suma Cum Laude* with honors) in electrical and biomedical engineering from Duke University, Durham, NC, USA, in 1990; the Ph.D. degree from the Department of Biomedical Engineering, The Johns Hopkins University, Baltimore, MD, USA, in 1998; and the M.D. degree from The Johns Hopkins University School of Medicine in 1998.

From 1991 to 1997, he conducted preclinical and human trials demonstrating the feasibility of retinal electrical stimulation in patients with Retinitis Pigmentosa, Wilmer Eye Institute, The Johns Hopkins Hospital, which led to the granting of the Ph.D. degree. He has served as a Lead Reviewer for IDEs and 510(k)s with the Office of Device Evaluation, US Food and Drug Administration, in the Neurological Devices Division, leading an investigation into the safety and efficacy of a class of neurological devices. He is a co-founder of Second Sight Medical Products, Inc., developer and marketer of the Argus II Retinal Prosthesis System and the Orion Cortical Prosthesis System. He is the Chairman of the Board of Directors with Second Sight Medical Products, Sylmar, CA; the Alfred Mann Foundation, Valencia, CA; and the Southern California Biomedical Council, Los Angeles, CA; and has served on the board of directors for Pulse Biosciences and Los Feliz Arts Charter. He has started several other small companies, including one called "Campus Securit," which designed, manufactured, and marketed an electronic intercom security system called TELEKEY. These intercoms have been used in every dormitory at Princeton University, Duke University, and several other universities across the United States. He has published more than 90 articles and is a named inventor on more than 400 global patents, including more than 200 issued US patents.

Dr. Greenberg is a member of the New York Academy of Sciences, a Fellow of the American Institute for Medical and Biological Engineering, and a Fellow of the National Academy of Inventors.

Gianluca Lazzi (S'94–M'95-SM'99–F'08) received the Dr.Eng. degree in electronics from the University of Rome La Sapienza, Rome, Italy, in 1994; the Ph.D. degree in electrical engineering from the University of Utah, Salt Lake City, UT, USA, in 1998; and the Executive M.B.A. degree, specialized in Corporate Finance, from IE Business School (Instituto de Empresa), Madrid, Spain, in 2015.

He is currently a Provost Professor of ophthalmology, electrical engineering, and clinical entrepreneurship with the University of Southern California, Los Angeles, CA, USA. Previously, he served as a USTAR Professor and Department Chair with the Department of Electrical and Computer Engineering, University of Utah, Salt Lake City, UT, USA, and the Director of the Engineering Entrepreneurship Certificate with the same institution. Prior to his appointment at the University of Utah, he was a Professor (2006–2009), an Associate Professor (2003–2006), and an Assistant Professor (1999–2003) with the Department of Electrical and Computer Engineering, North Carolina State University, Raleigh, NC, USA. He has authored or coauthored more than 200 international journal papers, conference presentations, and book chapters on implantable devices, medical applications of electromagnetics, wireless telemetry, antenna design, computational modeling, dosimetry, and bioelectromagnetics.

Dr. Lazzi was the Chair of Commission K (Electromagnetics in Biology and Medicine) (2006–2008) and a Member-at-Large (2009–2011) of the U.S. National Committee of the International Union of Radio Science (URSI). He was an Associate Editor for the IEEE ANTENNAS AND WIRELESS PROPAGATION LETTERS (2001–2007) and served as the Editor-in-Chief of the IEEE ANTENNAS AND WIRELESS PROPAGATION LETTERS from 2008 to 2013. He also served as a Guest Editor for the Special Issue on Biological Effects and Medical Applications of RF/Microwaves of the IEEE TRANSACTIONS ON MICROWAVE THEORY AND TECHNIQUES in 2004 and as the Technical Program Chair of the IEEE Antennas and Propagation International Symposium and URSI meeting in Charleston, SC, USA, in 2009. He served as a Member of the Editorial Board of the PROCEEDINGS OF THE IEEE, the Chair of the IEEE Sensors Council Fellow Committee, and the Chair of the Publications Committee of the IEEE AP Society. He currently serves as the VP Publications of the IEEE Sensors Council and as a member of the Editorial Board of IEEE ACCESS. In 2014, he was the General Co-Chair of the IEEE Microwave Symposium on RF and Wireless Technologies for Biomedical Applications. In 2015, he co-founded Teveri LLC, which is focused on the commercialization of liquid metal technology for textile and consumer electronics applications. He was the recipient of the 1996 Curtis Carl Johnson Memorial Award for the best student paper presented at the 18th Annual Technical Meeting of the Bioelectromagnetics Society, the 1996 URSI Young Scientist Award, the 2001 Whitaker Foundation Biomedical Engineering Grant for Young Investigators, the 2001 National Science Foundation CAREER Award, the 2003 NCSU Outstanding Teacher Award, the 2003 NCSU Alumni Outstanding Teacher Award, the 2003 ALCOA Foundation Engineering Research Award, the 2006 H.A. Wheeler Award from the IEEE Antennas and Propagation Society for the best application paper published in the IEEE TRANSACTIONS ON ANTENNAS AND PROPAGATION in 2005, the 2008 Best Paper Award at the IEEE GlobeCom Conference, the 2009 ALCOA Foundation Distinguished Engineering Research Award, the 2009 R&D 100 Award, and the 2009 Editors Choice Award from the R&D Magazine for the Artificial Retina Project.